Reciprocal regulation of two G protein-coupled receptors sensing extracellular concentrations of Ca^{2+} and H^+

Wei-Chun Wei, Benjamin Jacobs, Esther B. E. Becker, and Maike D. Glitsch[1]

Department of Physiology, Anatomy and Genetics, University of Oxford, Oxford OX1 3PT, United Kingdom

Edited by Robert J. Lefkowitz, Howard Hughes Medical Institute, Duke University Medical Center, Durham, NC, and approved July 10, 2015 (received for review March 27, 2015)

G protein-coupled receptors (GPCRs) are cell surface receptors that detect a wide range of extracellular messengers and convey this information to the inside of cells. Extracellular calcium-sensing receptor (CaSR) and ovarian cancer gene receptor 1 (OGR1) are two GPCRs that sense extracellular Ca^{2+} and H^+, respectively. These two ions are key components of the interstitial fluid, and their concentrations change in an activity-dependent manner. Importantly, the interstitial fluid forms part of the microenvironment that influences cell function in health and disease; however, the exact mechanisms through which changes in the microenvironment influence cell function remain largely unknown. We show that CaSR and OGR1 reciprocally inhibit signaling through each other in central neurons, and that this is lost in their transformed counterparts. Furthermore, strong intracellular acidification impairs CaSR function, but potentiates OGR1 function. Thus, CaSR and OGR1 activities can be regulated in a seesaw manner, whereby conditions promoting signaling through one receptor simultaneously inhibit signaling through the other receptor, potentiating the difference in their relative signaling activity. Our results provide insight into how small but consistent changes in the ionic microenvironment of cells can significantly alter the balance between two signaling pathways, which may contribute to disease progression.

OGR1 | pH sensing | extracellular acidosis | CaSR | microenvironment

Cells are surrounded by interstitial fluid, the composition of which is influenced by neighboring cells and which constitutes a key part of the microenvironment in which cells have to operate and survive. Changes in this microenvironment influence cell physiology (1, 2) and may promote disease (3, 4). Extracellular Ca^{2+} ($[Ca^{2+}]_o$) and H^+ ($[H^+]_o$) concentrations are important components of the microenvironment, and their extracellular concentration changes in an activity- and state-dependent manner (5, 6). $[Ca^{2+}]_o$ is required for membrane stability, serves as a reservoir to allow Ca^{2+} influx into cells, and contributes to the membrane potential. $[H^+]_o$ sets the local pH, thereby influencing protein function as well as contributing to the membrane potential. Furthermore, Ca^{2+} and H^+ can cross the membrane via ion channels and transporters, meaning that both can serve as intracellular and extracellular messengers (7–10).

Levels of $[Ca^{2+}]_o$ and $[H^+]_o$ are communicated to cells via cell surface receptors that change their activity in a manner dependent on $[Ca^{2+}]_o$ and $[H^+]_o$. These receptors include G protein-coupled receptors (GPCRs), such as the extracellular Ca^{2+}-sensing receptor (CaSR), ovarian cancer gene receptor 1 (OGR1), G protein-coupled receptor 4 (GPR4), and T-cell death-associated gene 8 (TDAG8), all of which sense $[H^+]_o$, as well as a range of ion channels (8).

Intriguingly, Ca^{2+} and H^+ signaling can be intimately linked, and changes in extracellular pH (pH_o) and intracellular pH (pH_i) may affect intracellular Ca^{2+} ($[Ca^{2+}]_i$) signaling directly and indirectly (8, 11, 12). This is exemplified by OGR1, which, like CaSR (13), can couple to G_q and hence trigger Ca^{2+} release from intracellular Ca^{2+} stores via activation of the phospholipase C pathway (14). Neither CaSR nor OGR1 desensitizes (13, 14); thus, they continually monitor $[Ca^{2+}]_o$ and $[H^+]_o$ levels, respectively, and faithfully report any changes in their extracellular concentration. Because of the vital importance of Ca^{2+} and H^+ to cells, information about their extracellular presence is crucial for cells, and lack of or altered signaling through these receptors may contribute to disease pathways.

We have previously found that OGR1 activation in DAOY cells, a human cerebellar granule cancer cell line, leads to complex $[Ca^{2+}]_i$ signals and activation of the ERK signaling pathway, thereby providing a mechanistic explanation of how the acidic environment may influence transformed cell function and/or survival (15). This action is lost on differentiation, suggesting a link between OGR1 activity and proliferative behavior of the transformed neurons (16). To better understand the role played by OGR1 in central neurons, we investigated OGR1 activation in primary cerebellar granule cells, the nontransformed equivalent of DAOY cells. We found that OGR1 and CaSR reciprocally inhibit $[Ca^{2+}]_i$ signaling through each other, and that intracellular acidosis, which accompanies extracellular acidification, promotes OGR1 but inhibits CaSR activity. Finally, CaSR-dependent inhibition of OGR1activity is absent in DAOY cells.

Results

We first established that OGR1 was expressed in primary wild-type (WT) murine cerebellar granule cell cultures throughout their culturing period [days in vitro (DIV) 2–15] using RT-PCR

Significance

The composition of the extracellular fluid surrounding all cells changes in an activity-dependent manner. Cell surface receptors allow cells to respond to components of the fluid, which is vital for proper functioning of cells and tissues. Ca^{2+} and H^+ are crucial for cell survival and functioning. Their extracellular concentrations are monitored by two receptors, extracellular calcium-sensing receptor (CaSR) and ovarian cancer gene receptor 1 (OGR1), respectively. We report that these two receptors can be regulated in a seesaw manner; conditions favoring activity of one receptor inhibit signaling through the other, and vice versa, allowing cells to detect subtle changes in the extracellular concentration of these ions. We provide evidence that dysregulated activity of CaSR and OGR1 may contribute to the formation and progression of pathologies.

Author contributions: W.-C.W., B.J., and M.D.G. designed research; W.-C.W. and B.J. performed research; E.B.E.B. contributed new reagents/analytic tools; W.-C.W., B.J., and M.D.G. analyzed data; and W.-C.W. and M.D.G. wrote the paper.

The authors declare no conflict of interest.

This article is a PNAS Direct Submission.

Freely available online through the PNAS open access option.

[1]To whom correspondence should be addressed. Email: maike.glitsch@dpag.ox.ac.uk.

This article contains supporting information online at www.pnas.org/lookup/suppl/doi:10.1073/pnas.1506085112/-/DCSupplemental.

(Fig. 1*A*). We next carried out fluorescence Ca^{2+} imaging experiments to see whether extracellular acidosis could trigger changes in $[Ca^{2+}]_i$ concentration. We first dropped pH_o from 8 to 6 in the absence of $[Ca^{2+}]_o$ but in the presence of 2 mM extracellular Mg^{2+} ($[Mg^{2+}]_o$) (Ca^{2+}-free conditions). Increases in $[Ca^{2+}]_i$ under these conditions reflect Ca^{2+} release from intracellular Ca^{2+} stores, suggesting functional OGR1 expression.

Results in response to extracellular acidification under Ca^{2+}-free conditions were very variable (Fig. S1); thus, we repeated the experiments in the presence of $Ca^{2+}{}_o$ to obtain more robust and reliable Ca^{2+} signals, as both Ca^{2+} release from stores and Ca^{2+} influx through plasma membrane channels should contribute to the overall fluorescence signal. However, extracellular acidification did not give rise to any change in $[Ca^{2+}]_i$ under these conditions (Fig. 1*B*), suggesting that the presence of $Ca^{2+}{}_o$ interfered with acidosis-mediated changes in $[Ca^{2+}]_i$ in granule cells.

We therefore considered that extracellular divalents might inhibit OGR1 signaling and repeated extracellular acidification experiments in the absence of $[Ca^{2+}]_o$ and $[Mg^{2+}]_o$ (in the additional presence of 0.1 mM EGTA and EDTA; divalent-free conditions). Under these conditions, we measured robust increases in $[Ca^{2+}]_i$ in all cells tested subsequent to extracellular acidification (Fig. 1*B*). Thus, $[Ca^{2+}]_o$ and $[Mg^{2+}]_o$ interfere with OGR1 signaling.

Both Ca^{2+} and Mg^{2+} are agonists of CaSR (13), and GPCRs have been documented to inhibit signaling through one another (17–19). Therefore, we considered the possibility that CaSR might inhibit OGR1 activity. To address this, we used two distinct pharmacologic inhibitors of CaSR, NPS2390 and NPS2143, and tested their impact on $[Ca^{2+}]_i$ signaling in the presence of $[Ca^{2+}]_o$ and $[Mg^{2+}]_o$, when CaSR is active. There was a prominent rise in $[Ca^{2+}]_i$ on extracellular acidification in the presence of these antagonists that was observed in all cells and that was larger than the Ca^{2+} signal in the absence of extracellular divalents (Fig. 1*B*), suggesting that extracellular acidosis can evoke Ca^{2+} influx and Ca^{2+} release from intracellular $Ca^{2+}{}_i$ stores.

Importantly, in the absence of $[Ca^{2+}]_o$ and $[Mg^{2+}]_o$, neither NPS2143 nor NPS2390 had any impact on the acidosis-mediated rise in $[Ca^{2+}]_i$ (Fig. S2), demonstrating selectivity of the inhibitors for CaSR.

To confirm a role for CaSR in inhibiting acidosis-mediated $[Ca^{2+}]_i$ signals, we used an shRNA internal ribosome entry site–red fluorescent protein (IRES-RFP) tag approach to knock down CaSR. In successfully transfected cells, extracellular acidosis triggered a rise in $[Ca^{2+}]_i$ in the presence of extracellular divalents (Fig. 1*C*) (extent of knockdown shown in Fig. S3 *A* and *B*). Thus, knockdown of CaSR led to disinhibition of acidosis-dependent $[Ca^{2+}]_i$ signaling in granule cells that was not observed in cells transfected with a control (scrambled) sh-construct (Fig. 1*C*). Fig. S3*C* lists the shScramble controls to demonstrate the specificity of the sh-CaSR approach.

CaSR is activated by $[Ca^{2+}]_o$ in the physiological range (0.1–1 mM) (13); therefore, we examined whether this was also the Ca^{2+} concentration range inhibiting acidosis-mediated Ca^{2+} signals. Under divalent-free conditions, extracellular acidification gave rise to a robust $[Ca^{2+}]_i$ signal, but already at 0.1 mM Ca^{2+}, the peak Ca^{2+} signal was reduced, and full block was observed at 1 mM $[Ca^{2+}]_o$ (Fig. 1 *D* and *E*). A 50% block of acidosis-mediated $[Ca^{2+}]_i$ signals was achieved in the presence of 0.36 mM $[Ca^{2+}]_o$ (Fig. 1*E*). Moreover, there was a significant delay in the time to peak of the $[Ca^{2+}]_i$ signal (Fig. 1 *D* and *F*; $P < 0.0001$).

We next wanted to establish whether the rises in $[Ca^{2+}]_i$ observed in granule cells in response to extracellular acidosis were mediated by OGR1, or whether there might be a role for other acid-sensing proteins in this process, by establishing granule cell cultures from *Ogr1* knockout (KO) mice (*Ogr1*$^{-/-}$). In these cells, extracellular acidification did not give rise to any changes in $[Ca^{2+}]_i$ even when CaSR activity was inhibited (Fig. 2*A*), demonstrating that the changes in $[Ca^{2+}]_i$ signaling observed in response to extracellular acidification in WT cells were not mediated by proteins other than OGR1.

To further prove this latter point, we introduce murine OGR1 (RFP-tagged) back into *Ogr1*$^{-/-}$ cells. This resulted in acidosis-dependent $Ca^{2+}{}_i$ signals in successfully transfected cells (Fig. 2*B*) that exhibited the same CaSR-mediated suppression of OGR1 signaling observed in WT cells (Figs. 1*B* and 2*B*). Extracellular acidosis-induced changes in $[Ca^{2+}]_i$ were not observed in *Ogr1*$^{-/-}$ cells transfected with an empty RFP vector control (Fig. S4).

We next determined the pH dependence of OGR1 activation in WT cells (divalent-free conditions). Dropping pH_o from 8 to 7.35 did not produce any appreciable increase in $[Ca^{2+}]_i$, but there was a significant rise in $[Ca^{2+}]_i$ at pH_o 6.8 and below ($P < 0.0001$; Fig. 2*C*). The peak $[Ca^{2+}]_i$ rises showed a clear dependence on

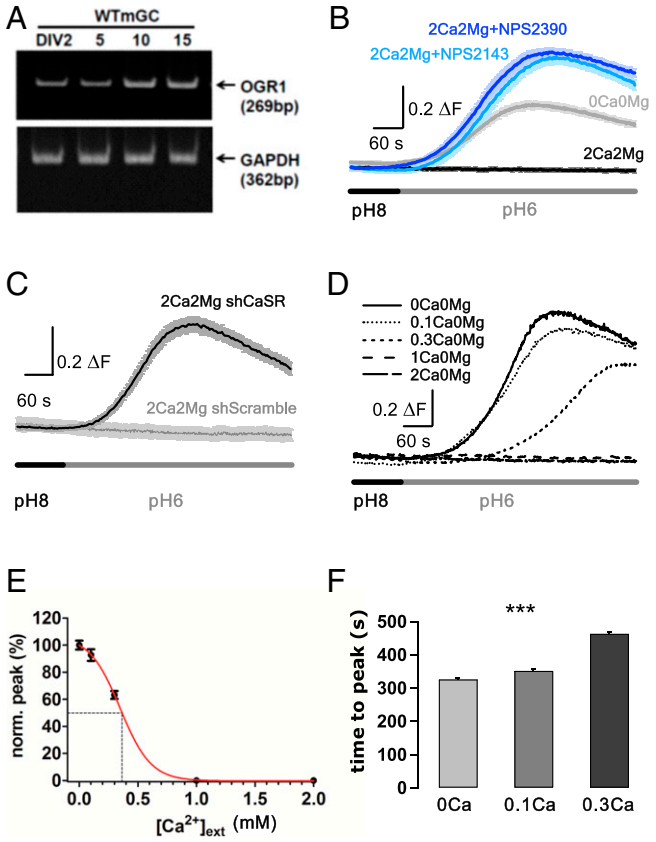

Fig. 1. CaSR inhibits extracellular acidification-mediated $[Ca^{2+}]_i$ signaling. (*A*) Murine cerebellar granule cells express OGR1 mRNA at different DIV stages. (*B*) Average fluorescence traces recorded in WT granule cells in response to extracellular acidification from pH 8 to pH 6 in the absence (0Ca0Mg) and presence of 2 mM $Ca^{2+}{}_o$ and $Mg^{2+}{}_o$ (2Ca2Mg), and in the additional presence of CaSR inhibitors 10 μM NPS2143 (2Ca2Mg+NPS2143) or NPS2390 (2Ca2Mg+NPS2390). n = 46–56 cells. (*C*) Average fluorescence traces in WT granule cells in response to extracellular acidification in the presence of extracellular divalents following knockdown of CaSR (shCaSR) and using a scrambled sh construct (shScrambled) as a negative control. n = 38–49 cells. (*D*) Representative raw traces showing the effects of extracellular acidification in presence of increasing $[Ca^{2+}]_o$ in WT granule cells. All experiments were performed in the absence of $[Mg^{2+}]_o$. (*E*) Average peak fluorescence signals in response to acidification from pH_o8–6 for a given $[Ca^{2+}]_o$ were normalized to average peak fluorescence signal at 0 mM $Ca^{2+}{}_o$ (taken as 100%). Experimental conditions were as in *D*. Dotted lines indicate the position of 50% of the control fluorescence signal at 0 mM $Ca^{2+}{}_o$. n = 85–92 cells. (*F*) Average time delay between extracellular acidification and peak response in presence of increasing $[Ca^{2+}]_o$, measured in seconds. Same cells as for *E*. ***$P < 0.0001$.

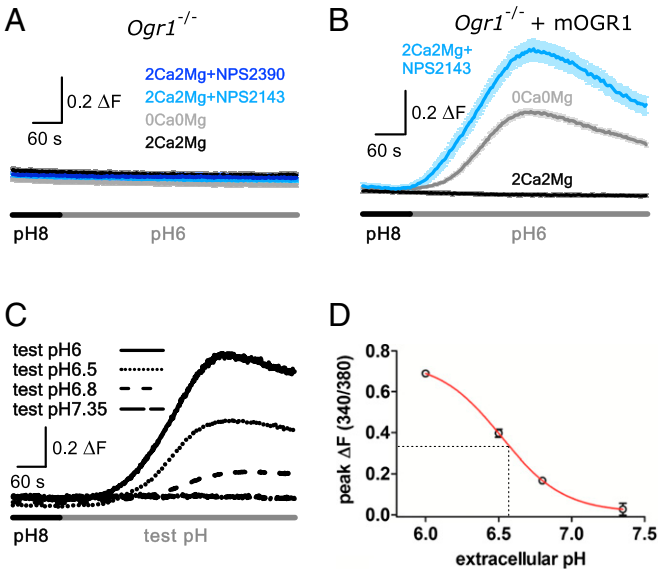

Fig. 2. OGR1 underlies the acidification-mediated $[Ca^{2+}]_i$ signaling. (*A*) Average fluorescence response to acidification from pH_o8–6 measured in *Ogr1*$^{-/-}$ granule cells in the absence (0Ca0Mg), and presence of 2 mM Ca^{2+}_o and Mg^{2+}_o (2Ca2Mg), and in the additional presence of NPS2143 (10 μM; 2Ca2Mg+NPS2143) or NPS2390 (10 μM; 2Ca2Mg+NPS2390). n = 46–56 cells. (*B*) The same experiments as in *A*, but following transfection of murine *Ogr1* into *Ogr1*$^{-/-}$ cells (*Ogr1*$^{-/-}$ + mOGR1). n = 26–49 cells. (*C*) Representative raw traces showing the dose–response curve of OGR1 signaling to extracellular acidosis in absence of extracellular divalent cations in WT granule cells. (*D*) Experiments performed as in *C*. Average peak Ca^{2+} signals were plotted against the pH_o at which they occurred. All data were obtained in WT granule cells. n = 47–53 cells. Dotted lines indicate the pH_o at which the measured response is one-half that measured at pH 6.

pH_o (Fig. 2*D*). Assuming maximal activation of OGR1 at pH_o 6, half-maximal activation of OGR1 in WT cells was achieved when pH_o dropped to around 6.6 (Fig. 2*D*). Furthermore, the kinetics also strongly depended on pH_o ($P < 0.0001$; Fig. S5). Thus, OGR1 in cerebellar granule cells has a more acidic pH dependence than has been reported previously for some cells (14, 15), but not for others (20, 21).

CaSR is inhibited by extracellular acidosis owing to pH effects on its agonist binding site (22); a role for OGR1 in influencing CaSR signaling was not considered in that study. Thus, we investigated whether OGR1 and CaSR could engage in reciprocal regulation by activating CaSR (increase in $[Ca^{2+}]_o$ from 0 to 2 mM in the absence of $[Mg^{2+}]_o$) at different pH_o values in WT and *Ogr1*$^{-/-}$ cells. There was a significant reduction in CaSR responsiveness with increasing extracellular acidification in both cell types (peak Ca^{2+} signal, B Ca^{2+} integral; $P < 0.0001$ for both; Fig. 3*A*). However, for almost every given pH_o value, the CaSR-mediated Ca^{2+} responses were smaller in WT cells than in *Ogr1*$^{-/-}$ cells ($P < 0.0002$).

The foregoing finding could reflect increased CaSR expression in *Ogr1*$^{-/-}$ cells compared with WT cells, thereby resulting in larger CaSR responses. Consequently, we compared CaSR protein expression levels in WT and *Ogr1*$^{-/-}$ DIV2 and DIV15 granule cells and found no difference in CaSR expression levels (Fig. 3 *C* and *D*).

Furthermore, at pH_o 8, CaSR responses were identical in WT and *Ogr1*$^{-/-}$ cells (Fig. 3 *A* and *B*). At this pH, OGR1 is not active (14), and WT cells should behave like *Ogr1*$^{-/-}$ cells, which is what we observed. Thus, the reduced CaSR responses in WT cells compared with *Ogr1*$^{-/-}$ cells is a likely consequence of OGR1 interfering with CaSR-mediated $[Ca^{2+}]_i$ signaling in WT cells.

Our data also show that the impact of OGR1 on CaSR-dependent signaling is not restricted to influencing peak Ca^{2+} signals. CaSR-mediated Ca^{2+} influx in WT was smaller than that in *Ogr1*$^{-/-}$ cells; this was particularly evident in the integral Ca^{2+} response at pH_o 6.8 and below (Fig. S6).

Extracellular acidification also may lead to (transient) intracellular acidification (15). To investigate whether this could contribute to the inhibition of CaSR-mediated signaling following extracellular acidification, we looked at pH_i changes in response to pH_o changes using fluorescence H^+ imaging with BCECF [2′,7′-Bis-(2-carboxyethyl)-5-(and-6)-carboxyfluorescein] as the H^+ dye. First, cells were exposed to different pH_o conditions for 5 min, and then pH_i was measured. A clear dependence of pH_i on pH_o was seen; the more acidic the pH_o, the more acidic the pH_i, albeit to a lesser extent (Fig. S7*A*).

To study impact of intracellular acidosis on CaSR function, we induced intracellular acidification in the absence of extracellular acidification using different concentrations of extracellular sodium acetate ($[NaAc]_o$) (15, 23) (Fig. S7*B*). These experiments showed that 25 and 50 mM $[NaAc]_o$ produced the same intracellular acidification as an extracellular acidification to pH 6 (Fig. S7*C*). Thus, the use of 25 or 50 mM NaAc mimics intracellular acidification in response to extracellular acidification to pH 6.

Finally, we determined whether WT and *Ogr1*$^{-/-}$ granule cells showed the same changes in pH_i in response to extracellular acidification. OGR1 reportedly affects pH_i regulation (24), and lack of OGR1 expression in *Ogr1*$^{-/-}$ cells might affect the cells' ability to handle $[H^+]_i$, resulting in variations in intracellular acidification. This could then affect CaSR function, thereby explaining some of the disparities in CaSR responses observed between WT and *Ogr1*$^{-/-}$ cells.

Consequently, we compared levels of intracellular acidification to acute extracellular acidification in WT and *Ogr1*$^{-/-}$ cells and found no differences (Fig. S7*D*). Thus, differences in extent of inhibition of CaSR by extracellular acidosis in WT cells vs.

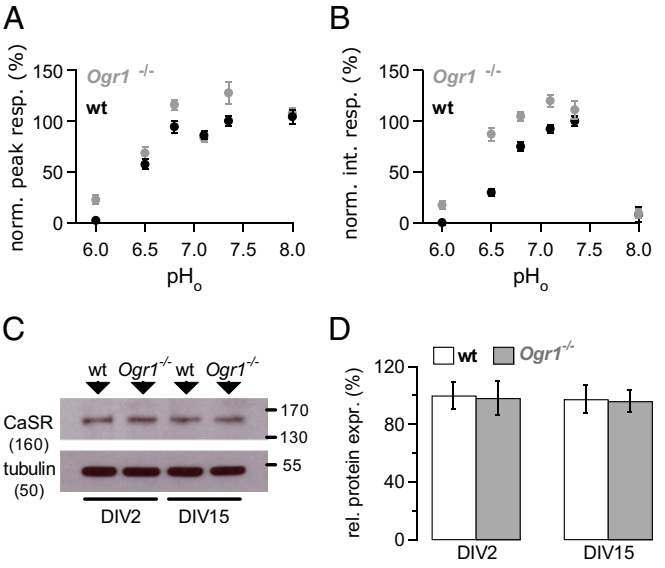

Fig. 3. CaSR is subject to inhibition by OGR1. (*A*) Averaged peak fluorescence responses following activation of CaSR by increasing $[Ca^{2+}]_o$ from 0 to 2 mM at varying pH_o values. All data points are normalized to the average peak WT response at pH 7.35. n = 39–108 cells. (*B*) Data points depicting the integral (int.) of the CaSR response. Same cells and experiments as in *A*. All data points are normalized to the average integral response in WT at pH7.35. (*C*) Western blot of CaSR expression in WT and *Ogr1*$^{-/-}$ granule cells at DIV2 and 15. α–tubulin served as an internal control. Molecular weights are given in kDa. (*D*) Average relative (rel.) CaSR protein expression (expr.) level. All values are normalized to the average CaSR expression in WT granule cell cultures at DIV2. n = 2 repeats per condition.

Ogr1$^{-/-}$ cells are unlikely to result from varying degrees of intracellular acidification.

We next studied the impact of intracellular acidosis on CaSR-dependent Ca^{2+} signaling in WT cells to assess the possible contribution of this to the decreased CaSR responses measured on extracellular acidification. We studied CaSR activation in response to increasing $[Ca^{2+}]_o$ from 0 to 2 mM under control conditions (at pH_o 8) and under conditions of intracellular acidification (+ 25 mM NaAc, at pH_o 8). There was a clear change in the time course of the CaSR response under conditions of intracellular acidosis (Fig. 4*A*); the response was slower to develop and displayed a smaller peak and plateau phase. Thus, intracellular acidification interferes with CaSR-dependent signaling independent of extracellular acidosis. CaSR is not the only GPCR affected by intracellular acidosis, however; we also found inhibited signaling ability of metabotropic ATP receptors P2Y1 and 6 under conditions of intracellular acidosis (Fig. S8).

Taken together, our findings indicate that neither OGR1-dependent inhibition of CaSR, nor intracellular acidification can fully explain the large extent of inhibition of CaSR observed at pH_o 6. This suggests that extracellular acidosis inhibits CaSR by changing its agonist responsiveness (22), via activation of OGR1, and by causing intracellular acidosis.

We next wanted to establish whether or not OGR1 is also subject to modulation of its signaling ability by intracellular acidosis. The idea is that OGR1 should not be inhibited by intracellular acidification, given that this can accompany extracellular acidosis, which activates OGR1. Therefore, we considered that intracellular acidification might in fact promote OGR1 signaling.

As shown in Fig. 2*C*, a drop in pH_o from 8 to 7.35 did not result in any consistent Ca^{2+} responses in these cells, despite the fact that OGR1 is partially active at pH_o 7.35 (14). Thus, to investigate the impact of intracellular acidification on OGR1, we carried out experiments (under divalent-free conditions) in WT cells at pH_o 7.35, where OGR1 is partially active, in which we acidified pH_i using NaAc and monitored $[Ca^{2+}]_i$. The idea was that if OGR1 were potentiated at this permissive pH_o, then we should see changes in $[Ca^{2+}]_i$ in response to intracellular acidification owing to increased OGR1 activity.

In these experiments, we indeed saw a distinct rise in $[Ca^{2+}]_i$ in WT cells on intracellular acidification at pH_o 7.35 (Fig. 4*B*) that was not observed at pH_o 8, where OGR1 is not active (Fig. 4*C*). Furthermore, there was no rise in $[Ca^{2+}]_i$ in *Ogr1*$^{-/-}$ cells in response to intracellular acidification at pH_o 7.35 (Fig. 4*D*). This demonstrates that the $[Ca^{2+}]_i$ rise observed in WT cells at pH_o 7.35 upon intracellular acidification was related to increased OGR1 activity.

Crucially, the foregoing results confirm that intracellular acidosis inhibits CaSR signaling by acting on CaSR directly. The smaller Ca^{2+} rises in response to CaSR activation under conditions of intracellular acidification could have been the result of pH_i effects on the signaling cascades downstream of G_q activation; however, if this were the case, then OGR1 signaling should be equally impaired by intracellular acidosis. Our results show that the opposite is the case, suggesting that intracellular acidosis affects CaSR and OGR1 directly.

Given that intracellular acidosis can inhibit CaSR and promote OGR1 function, and CaSR inhibits signaling through OGR1, we wondered whether intracellular acidic preconditioning might alleviate CaSR-mediated inhibition of OGR1 function. Reduced CaSR activity and/or increased OGR1 signaling ability might permit OGR1 to signal even when CaSR is active. To address this question, we exposed WT cells (Fig. 4*E*) and *Ogr1*$^{-/-}$ cells (Fig. 4*F*) to (*i*) a pH_o change from 8 to 6 only, (*ii*) intracellular acidification at constant pH_o 8 (using NaAc) only, and (*iii*) intracellular acidification followed by extracellular acidification. All experiments were carried out in the presence of extracellular divalents, to activate CaSR.

On acidification of pH_o only, there was no obvious change in $[Ca^{2+}]_i$ in WT or *Ogr1*$^{-/-}$ cells (Fig. 4 *E* and *F*, black). Following intracellular acidification only, there was a small rise in $[Ca^{2+}]_i$ (Fig. 4 *E* and *F*, purple), which was also present in previous experiments (Fig. 4 *C* and *D*) and was independent of OGR1, given that it was also seen at pH_o 8 and in *Ogr1*$^{-/-}$ cells. However, when intracellular acidification preceded extracellular acidification, we observed a further clear increase in $[Ca^{2+}]_i$ in WT cells, but not in *Ogr1*$^{-/-}$ cells (Fig. 4 *E* and *F*, green). This demonstrates that intracellular acidosis can increase OGR1 function by reducing CaSR and/or promoting OGR1 signaling ability.

Our original research into OGR1 was carried out in DAOY cells, in which H^+-induced currents in response to OGR1 activation were recorded in the presence of extracellular divalents (15), suggesting that OGR1 is not subject to inhibition by CaSR in these cells. To confirm this, we carried out fluorescence Ca^{2+} imaging experiments in DAOY cells in the presence of $[Ca^{2+}]_o$ and $[Mg^{2+}]_o$ and found that under these conditions, a drop in pH_o to 6 did indeed trigger a rise in $[Ca^{2+}]_i$ in virtually all cells

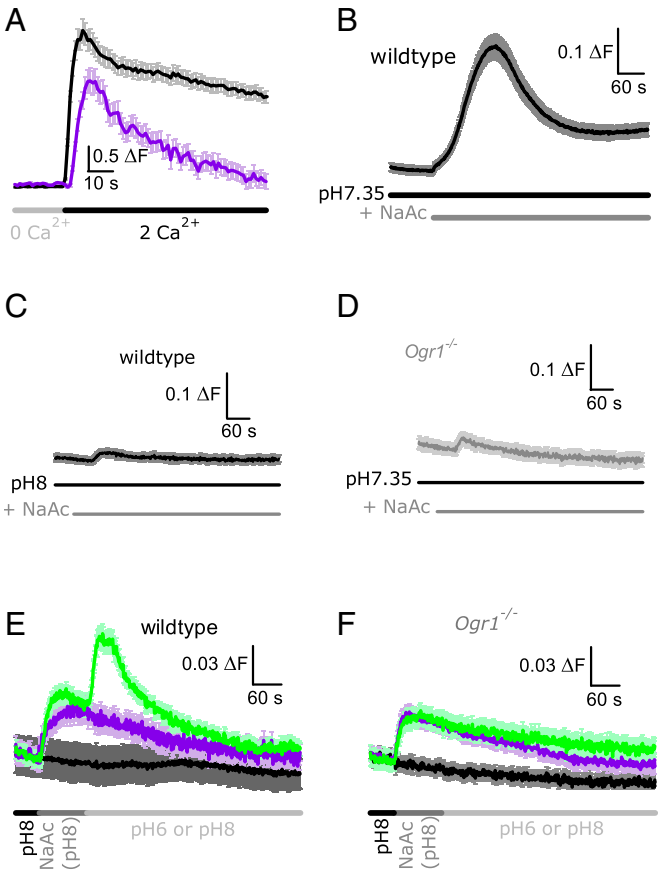

Fig. 4. Intracellular acidosis inhibits CaSR and potentiates OGR1. (*A*) Average (± SEM) CaSR fluorescence responses at pH_o8 under control conditions (black) and following intracellular acidification with 25 mM NaAc (purple). n = 30–37 cells. Responses were evoked by increasing $[Ca^{2+}]_o$ from 0 to 2 mM (in the absence of $[Mg^{2+}]_o$). (*B*) Average graph showing the impact of intracellular acidification by 50 mM NaAc at extracellular pH 7.35 in the presence of extracellular divalents and 10 μM NPS2390 in WT cells (n = 52). (*C* and *D*) Same experimental protocol as for *B*, but either at pH_o 8 in WT granule cells (n = 27) (*C*) or using *Ogr1*$^{-/-}$granule cells (n = 27) (*D*). (*E*) Black, pH_o 8 acidified to pH_o 6 after 150 s. Purple, pH_o 8 constant and pH_i acidified with 50 mM sodium acetate after 50 s. Green, pH_i acidified with 50 mM sodium acetate after 50 s (pH_o 8), and pH_o acidified to 6 after 150 s. n = 66–74 cells. (*F*) Same experiments as in *E*, but carried out in *Ogr1*$^{-/-}$ granule cells. n = 31–45 cells.

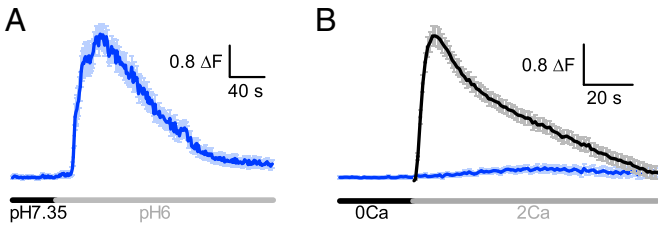

Fig. 5. Transformed granule cells lack CaSR-mediated inhibition of OGR1-dependent $[Ca^{2+}]_i$ signals and reduced CaSR signaling activity. (*A*) Average data (±SEM) for OGR1-mediated intracellular fluorescence change in DAOY cells ($n = 30$ cells) in response to extracellular acidification from pH 7.35–6; experiments in the presence of divalents. (*B*) Average graphs (± SEM) showing CaSR responses in DAOY (blue; $n = 46$) and WT granule cells (black; $n = 67$). All experiments were done in the absence of $[Mg^{2+}]_o$.

tested (Fig. 5*A*), indicating OGR1 activation. These results suggest that CaSR does not interfere with OGR1 in DAOY cells, whether through lack of functional expression or through any other (additional) mechanism.

We then examined functional CaSR expression in DAOY cells by increasing $[Ca^{2+}]_o$ from 0 to 2 mM (in the absence of $[Mg^{2+}]_o$) at pH_o 8 (to prevent a potential impact of OGR1 on CaSR). Following this protocol, we observed a small and slow rise in $[Ca^{2+}]_i$ in response to CaSR activation that was much smaller than the Ca^{2+} rise seen in primary WT granule cells subjected to the same experimental procedure (Fig. 5*B*). Thus, DAOY cells do express functional CaSRs, but their level of activity is lower than that in their nontransformed counterparts.

Discussion

We show that in central neurons, two GPCRs (CaSR and OGR1) that sense extracellular concentrations of physiologically relevant ions (Ca^{2+} and H^+, respectively) can control each other's signaling activity. Thus, the activity of one receptor may profoundly influence the signaling ability of the other receptor. We also show that intracellular acidification, which may accompany extracellular acidosis, inhibits CaSR responses but potentiates OGR1 responses. The impact of intracellular acidosis on signaling ability is not limited to CaSR and OGR1; other receptors are affected by it as well.

Furthermore, our experimental conditions do not allow for cells to regulate their pH_i via the bicarbonate/CO_2 buffering system. The presence of this physiologically relevant buffering system would limit the extent of intracellular acidification in terms of spread, duration, and severity. Therefore, the observed opposite regulation of CaSR and OGR1 in response to intracellular acidification will be less prominent in the presence of the bicarbonate/CO_2 buffering system than in its absence.

The seesaw manner of CaSR and OGR1 regulation, whereby conditions promoting the activity of one receptor directly and indirectly inhibit that of the other receptor, may allow cells to monitor and respond to changes in environmental ion composition with exquisite sensitivity. The delicate reciprocity between CaSR and OGR1 signaling could explain why subtle changes in microdomain ion concentrations can disrupt intracellular signaling sufficiently to promote the development and amplification of pathological signaling pathways. Notably, CaSR activity is determined not only by the availability of its ligands (with Ca^{2+} the main physiological agonist), but also by its cell surface expression. Changes in this will lead to a reduction in CaSR-mediated signaling even in the absence of changes in $[Ca^{2+}]_o$ (25). Therefore, increased OGR1 activity may occur even when $[Ca^{2+}]_o$ is constant and/or at physiological levels.

Global $[Ca^{2+}]_o$ and $[H^+]_o$ are thought to be relatively stable, but their levels fluctuate in response to ion channel, transporter, metabolic, and functional activity in the cellular microenvironment (5, 6, 13). This is particularly true for the brain: Opening of Ca^{2+}-permeable ion channels during synaptic transmission leads to a temporary decease in local $[Ca^{2+}]_o$ (13, 26), whereas release of the neurotransmitter vesicular content into the synaptic cleft causes a decrease in pH_o (27). Furthermore, opening of $GABA_A$ channels, which are permeable to both Cl^- and HCO_3^-, may contribute to fluctuations in pH (28, 29). Because neither receptor desensitizes, they continuously communicate changes in $[Ca^{2+}]$ and $[H^+]$ to the cells in which they are expressed. Thus, the relative activity of these two receptors could be used by neurons and other cell types as a dynamic readout of the precise composition of the extracellular ionic milieu.

DAOY cells provide a model of transformed, malignant granule cells. We demonstrate that OGR1- and CaSR-dependent $[Ca^{2+}]_i$ signaling is altered in these cells. In fact, $[Ca^{2+}]_i$ signaling through OGR1 and CaSR appears to be opposite in the two cell types; in normal granule cells, OGR1-dependent $[Ca^{2+}]_i$ signaling is slow and small, whereas CaSR-dependent $[Ca^{2+}]_i$ signaling is fast and large, whereas the opposite is seen for DAOY cells. The lack of inhibition of OGR1 signaling by CaSR in DAOY cells is likely due, at least in part, to low functional expression levels of CaSR in these cells, given that knockdown of CaSR in granule cells also leads to disinhibition of OGR1 signaling.

Expression of OGR1 in the brain has been reported (30), but the spatiotemporal expression profile has not been well characterized. Much more is known about CaSR expression and function in the brain. CaSR is expressed in a number of distinct cell types throughout the brain, including neurons (31), and is thought to play a key role in development of the brain, synaptic transmission, and plasticity (32). Moreover, it has been implicated in brain pathologies, such as ischemia, neurodegenerative disease, and brain tumors (32). Intriguingly, these conditions are accompanied by extracellular acidosis (8, 33–36). OGR1 is functionally expressed in brain tumor cells (15), and changes in its activity levels may be relevant in other acidosis-accompanied pathological states. Thus, both OGR1 and CaSR have been implicated in brain disorders that are exacerbated by changes in $[H^+]_o$ and $[Ca^{2+}]_o$ (37). Dysregulation of the balance between OGR1 and CaSR signaling may contribute to the development and progression of wide-ranging pathological states.

CaSR and OGR1 also are coexpressed in a number of other tissues, including kidney (24, 30, 38), bone (13, 14, 20, 39, 40), and lung (30, 41–44). These tissues also experience extracellular acidification under physiological conditions. Intriguingly, both receptors have been implicated in diseases arising in these tissues (39–46), suggesting that altered signaling through CaSR and OGR1 may have a significant impact on disease progression in tissues other than the brain.

Materials and Methods

Cell Cultures. The cerebellar granule cell experiments were carried out using granule cell cultures derived from C57BL/6 WT mice (Charles River Laboratories) and *Ogr1* (C57BL/6 background) KO mice and cultured for up to 15 d (47). The *Ogr1* KO mice were a generous gift from K. Seuwen and T. Suply (Novartis). DAOY cells (American Type Culture Collection) were grown and cultured as described previously (15).

Fluorescence Imaging Experiments. The fluorescence Ca^{2+} imaging experiments and solutions have been described previously (15). All solutions were made using HPLC-grade water. Fura 2-AM and BCECF-AM were purchased from Molecular Probes-Invitrogen. Fluorescence ratios were recorded every 1 s for Fura 2-AM (340 nm/380 nm) and every 5 s for BCECF-AM (490 nm/439 nm); emission was measured at 535 nm. Preincubation was done for 30 min at room temperature with BCECF-AM (10 μM), and for 45 min at room temperature with Fura 2-AM in standard extracellular buffer at pH 7.35. The 490 nm/439 nm ratio was converted to a pH value using a calibration curve, obtained by measuring the fluorescence ratio in cells incubated in a high-K^+

solution at a pH range of 6.0–8.0 (four values) supplemented with nigericin (2 μM; Sigma-Aldrich) (48). Experimental conditions are described in detail in *SI Materials and Methods*. General chemicals for making solutions were obtained from Sigma-Aldrich.

RNA Extraction and RT-PCR. Total RNA from cultured mouse cerebellar granule cells and DAOY cells were extracted using a Qiagen RNeasy MiniKit according to the manufacturer's protocol. For RT-PCR, first-strand cDNA was synthesized from 1 μg of total RNA with an oligo-dT primer and the Moloney murine leukemia virus reverse transcriptase (Promega) according to the manufacturer's protocol. PCR reactions were optimized to 95 °C for 5 min, 30 amplification cycles for OGR1, and 20 amplification cycles for GAPDH at 95 °C for 30 s, 56 °C for 30 s, 72 °C for 30 s, and a final extension of 5 min at 72 °C. Primer sequences are presented in *SI Materials and Methods*.

Plasmids and Transfection. Plasmids containing the RFP-tagged full-length cDNA of murine OGR1, CaSR shRNA, or control scrambled shRNA (Origene) were transfected into cerebellar granule cells using the Amaxa Nucleofector 2b electroporation system (Lonza) according to the manufacturer's instructions. Cells were used at 48 h after transfection. Only transfected cells, selected on the basis of their RFP-dependent fluorescence properties, were used for experiments.

Analysis and Data Presentation. Fluorescence traces were analyzed offline using Igor Wavemetrics 3.14. Data are shown as average ± SEM. InStat 2.03 for Mackintosh was used for statistical analysis. ANOVA was performed for comparison of more than two averages, and the unpaired Student *t* test was used for comparison of two averages. For Figs. 1*E* and 2*D*, data were fitted with a sigmoidal dose–response equation using GraphPad Prism. All experiments were carried out on at least two separate preparations.

ACKNOWLEDGMENTS. We thank Drs. Klaus Seuwen and Thomas Suply for the *Ogr1* KO mouse and Professors Gero Miesenböck, Anant Parekh, and Robert Wilkins for helpful comments on this manuscript. This work was supported by Biotechnology and Biological Sciences Research Council Grant BB/1008748/1. E.B. is the recipient of a Research Fellowship from the Royal Society.

1. Lavin Y, et al. (2014) Tissue-resident macrophage enhancer landscapes are shaped by the local microenvironment. *Cell* 159(6):1312–1326.
2. Gosselin D, et al. (2014) Environment drives selection and function of enhancers controlling tissue-specific macrophage identities. *Cell* 159(6):1327–1340.
3. Quail DF, Joyce JA (2013) Microenvironmental regulation of tumor progression and metastasis. *Nat Med* 19(11):1423–1437.
4. Hussell T, Bell TJ (2014) Alveolar macrophages: Plasticity in a tissue-specific context. *Nat Rev Immunol* 14(2):81–93.
5. DeCoursey TE (2013) Voltage-gated proton channels: Molecular biology, physiology, and pathophysiology of the H(V) family. *Physiol Rev* 93(2):599–652.
6. Stock C, et al. (2007) pH nanoenvironment at the surface of single melanoma cells. *Cell Physiol Biochem* 20(5):679–686.
7. D Burgoyne R (2004) The neuronal calcium-sensor proteins. *Biochim Biophys Acta* 1742(1-3):59–68.
8. Glitsch M (2011) Protons and Ca^{2+}: Ionic allies in tumor progression? *Physiology (Bethesda)* 26(4):252–265.
9. Chakravarti B, Chattopadhyay N, Brown EM (2012) Signaling through the extracellular calcium-sensing receptor (CaSR). *Adv Exp Med Biol* 740:103–142.
10. Yáñez M, Gil-Longo J, Campos-Toimil M (2012) Calcium-binding proteins. *Adv Exp Med Biol* 740:461–482.
11. Wakabayashi I, Poteser M, Groschner K (2006) Intracellular pH as a determinant of vascular smooth muscle function. *J Vasc Res* 43(3):238–250.
12. Rizzuto R, De Stefani D, Raffaello A, Mammucari C (2012) Mitochondria as sensors and regulators of calcium signalling. *Nat Rev Mol Cell Biol* 13(9):566–578.
13. Brown EM, MacLeod RJ (2001) Extracellular calcium sensing and extracellular calcium signaling. *Physiol Rev* 81(1):239–297.
14. Ludwig MG, et al. (2003) Proton-sensing G-protein–coupled receptors. *Nature* 425(6953):93–98.
15. Huang WC, Swietach P, Vaughan-Jones RD, Ansorge O, Glitsch MD (2008) Extracellular acidification elicits spatially and temporally distinct Ca^{2+} signals. *Curr Biol* 18(10):781–785.
16. Huang WC, Swietach P, Vaughan-Jones RD, Glitsch MD (2009) Differentiation impairs low pH-induced Ca^{2+} signaling and ERK phosphorylation in granule precursor tumour cells. *Cell Calcium* 45(4):391–399.
17. Pao CS, Benovic JL (2002) Phosphorylation-independent desensitization of G protein-coupled receptors? *Sci STKE* 2002(153):pe42.
18. Ligeti E, Csépányi-Kömi R, Hunyady L (2012) Physiological mechanisms of signal termination in biological systems. *Acta Physiol (Oxf)* 204(4):469–478.
19. Butcher AJ, Kong KC, Prihandoko R, Tobin AB (2012) Physiological role of G-protein coupled receptor phosphorylation. *Handbook Exp Pharmacol* 208(208):79–94.
20. Pereverzev A, et al. (2008) Extracellular acidification enhances osteoclast survival through an NFAT-independent, protein kinase C-dependent pathway. *Bone* 42(1):150–161.
21. Tomura H, et al. (2005) Prostaglandin I(2) production and cAMP accumulation in response to acidic extracellular pH through OGR1 in human aortic smooth muscle cells. *J Biol Chem* 280(41):34458–34464.
22. Quinn SJ, Bai M, Brown EM (2004) pH Sensing by the calcium-sensing receptor. *J Biol Chem* 279(36):37241–37249.
23. Sun B, Leem CH, Vaughan-Jones RD (1996) Novel chloride-dependent acid loader in the guinea-pig ventricular myocyte: part of a dual acid-loading mechanism. *J Physiol* 495(Pt 1):65–82.
24. Mohebbi N, et al. (2012) The proton-activated G protein-coupled receptor OGR1 acutely regulates the activity of epithelial proton transport proteins. *Cell Physiol Biochem* 29(3-4):313–324.
25. Bouschet T, Martin S, Henley JM (2008) Regulation of calcium-sensing receptor trafficking and cell-surface expression by GPCRs and RAMPs. *Trends Pharmacol Sci* 29(12):633–639.
26. Vassilev PM, Mitchel J, Vassilev M, Kanazirska M, Brown EM (1997) Assessment of frequency-dependent alterations in the level of extracellular Ca^{2+} in the synaptic cleft. *Biophys J* 72(5):2103–2116.
27. Traynelis SF, Chesler M (2001) Proton release as a modulator of presynaptic function. *Neuron* 32(6):960–962.
28. Kaila K, Voipio J (1987) Postsynaptic fall in intracellular pH induced by GABA-activated bicarbonate conductance. *Nature* 330(6144):163–165.
29. Chen JC, Chesler M (1990) A bicarbonate-dependent increase in extracellular pH mediated by $GABA_A$ receptors in turtle cerebellum. *Neurosci Lett* 116(1-2):130–135.
30. Xu Y, Casey G (1996) Identification of human OGR1, a novel G protein-coupled receptor that maps to chromosome 14. *Genomics* 35(2):397–402.
31. Yano S, Brown EM, Chattopadhyay N (2004) Calcium-sensing receptor in the brain. *Cell Calcium* 35(3):257–264.
32. Ruat M, Traiffort E (2013) Roles of the calcium sensing receptor in the central nervous system. *Best Pract Res Clin Endocrinol Metab* 27(3):429–442.
33. Jhala SS, Hazell AS (2011) Modeling neurodegenerative disease pathophysiology in thiamine deficiency: Consequences of impaired oxidative metabolism. *Neurochem Int* 58(3):248–260.
34. Damaghi M, Wojtkowiak JW, Gillies RJ (2014) pH sensing and regulation in cancer. *Front Physiol* 17:370.
35. Justus CR, Dong L, Yang LV (2013) Acidic tumor microenvironment and pH-sensing G protein-coupled receptors. *Front Physiol* 4:354.
36. McVicar N, et al. (2014) Quantitative tissue pH measurement during cerebral ischemia using amine and amide concentration-independent detection (AACID) with MRI. *J Cereb Blood Flow Metab* 34(4):690–698.
37. Kingsley LA, Fournier PGJ, Chirgwin JM, Guise TA (2007) Molecular biology of bone metastasis. *Mol Cancer Ther* 6(10):2609–2617.
38. Wagner CA (2013) The calcium-sensing receptor directly regulates proximal tubular functions. *Kidney Int* 84(2):228–230.
39. Yang M, et al. (2006) Expression of and role for ovarian cancer G-protein–coupled receptor 1 (OGR1) during osteoclastogenesis. *J Biol Chem* 281(33):23598–23605.
40. Li H, et al. (2009) Abnormalities in osteoclastogenesis and decreased tumorigenesis in mice deficient for ovarian cancer G protein-coupled receptor 1. *PLoS One* 4(5):e5705.
41. Ichimonji I, et al. (2010) Extracellular acidification stimulates IL-6 production and Ca(2+) mobilization through proton-sensing OGR1 receptors in human airway smooth muscle cells. *Am J Physiol Lung Cell Mol Physiol* 299(4):L567–L577.
42. Matsuzaki S, et al. (2011) Extracellular acidification induces connective tissue growth factor production through proton-sensing receptor OGR1 in human airway smooth muscle cells. *Biochem Biophys Res Commun* 413(4):499–503.
43. Saxena H, et al. (2012) The GPCR OGR1 (GPR68) mediates diverse signalling and contraction of airway smooth muscle in response to small reductions in extracellular pH. *Br J Pharmacol* 166(3):981–990.
44. Peng X, et al. (2014) Involvement of calcium-sensing receptors in hypoxia-induced vascular remodeling and pulmonary hypertension by promoting phenotypic modulation of small pulmonary arteries. *Mol Cell Biochem* 396(1-2):87–98.
45. Ward BK, Magno AL, Walsh JP, Ratajczak T (2012) The role of the calcium-sensing receptor in human disease. *Clin Biochem* 45(12):943–953.
46. Brown EM (2013) Role of the calcium-sensing receptor in extracellular calcium homeostasis. *Best Pract Res Clin Endocrinol Metab* 27(3):333–343.
47. Bilimoria PM, Bonni A (2008) Cultures of cerebellar granule neurons. *CSH Protoc* 2008:t5107.
48. Thomas JA, Buchsbaum RN, Zimniak A, Racker E (1979) Intracellular pH measurements in Ehrlich ascites tumor cells utilizing spectroscopic probes generated in situ. *Biochemistry* 18(11):2210–2218.